

# Processing Map for Hot Working of Metals

---

When a metallic alloy is subjected to deformation at high temperatures, it may undergo microstructural changes through different mechanisms. Some of these (e.g., dynamic recrystallisation and dynamic recovery) are known to be “safe” mechanisms, while others (e.g., void formation and wedge cracking) lead to the formation of defects.<sup>[1]</sup> Processing maps depict the hot workability of an alloy, by combining information about the ease with which its microstructure changes upon deformation with delineated regions of unstable flow. As such, they can be a useful tool to assess the ideal processing conditions that ensure a defect-free final product.<sup>[1,2]</sup> This report provides an overview of the model used in JMatPro® to calculate processing maps from flow stress data.

## Power Dissipation Map

Processing maps are calculated in the framework of the dynamic materials model,<sup>[1-3]</sup> whereby the metallic alloy in the hot working process (i.e., the workpiece) is described as a nonlinear dissipator. Crucially, the power absorbed during plastic flow is written as a sum of two explicit functions of the flow stress,  $\sigma$ , and strain rate,  $\dot{\epsilon}$ :<sup>[1-3]</sup>

$$P = G + J = \int_0^{\dot{\epsilon}} \sigma d\dot{\epsilon} + \int_0^{\sigma} \dot{\epsilon} d\sigma = \sigma \dot{\epsilon} \quad (1)$$

The first integral,  $G$ , known as the dissipator content, describes the power dissipated into heat, while  $J$ , the dissipator co-content, is related to microstructural changes in the workpiece.<sup>[1,2]</sup> Usually,  $G \geq J$ , and the maximum co-content is obtained for a linear dissipator:<sup>[1-3]</sup>

$$J_{max} = \frac{\sigma \dot{\epsilon}}{2} \quad (2)$$

The efficiency of power dissipation is then defined as the ratio<sup>[3]</sup>

$$\eta = \frac{J}{J_{max}} = 2 \left( 1 - \frac{1}{\sigma \dot{\epsilon}} \int_0^{\dot{\epsilon}} \sigma d\dot{\epsilon} \right) \quad (3)$$

The above quantity represents the ability of the workpiece to change its microstructure upon deformation. It may be derived entirely from flow stress data, either measured experimentally or calculated from suitable models. By plotting isovalue contours of  $\eta$  as a function of temperature,  $T$ , and strain rate, a power dissipation map is obtained.<sup>[1-3]</sup> This forms the first part of a processing map.

## Instability Criteria

The mechanisms that produce defect-free microstructures during high-temperature deformation, namely dynamic recrystallisation, superplasticity, and dynamic recovery,<sup>[1]</sup> are associated with high efficiency of power dissipation.<sup>[2]</sup> However, such is also the case for the detrimental mechanisms of void formation and wedge cracking.<sup>[1,2]</sup> A power dissipation map alone is, thus, insufficient to fully characterise the hot working behaviour of an alloy. In order to achieve this and, in particular, to optimise the processing parameters, it is important to distinguish those undesirable regions of unstable flow. By using appropriate instability criteria,<sup>[3,4]</sup> it is possible to identify such regions and build an instability map, which when superimposed on the isoefficiency contours results in the final processing map.<sup>[1-3]</sup>

Instability criteria may be established under a number of different assumptions. A common route is to apply stability concepts from Ziegler's plasticity theory to the dissipation functions of the dynamic materials model. This approach leads to the Kumar-Prasad and Murty-Rao criteria,<sup>[3,4]</sup> respectively given by

$$\xi_{K-P} = \frac{\partial \ln(m/(m+1))}{\partial \ln \dot{\epsilon}} + m < 0 \quad (4)$$

and

$$\xi_{M-R} = 2m - \eta < 0 \quad (5)$$

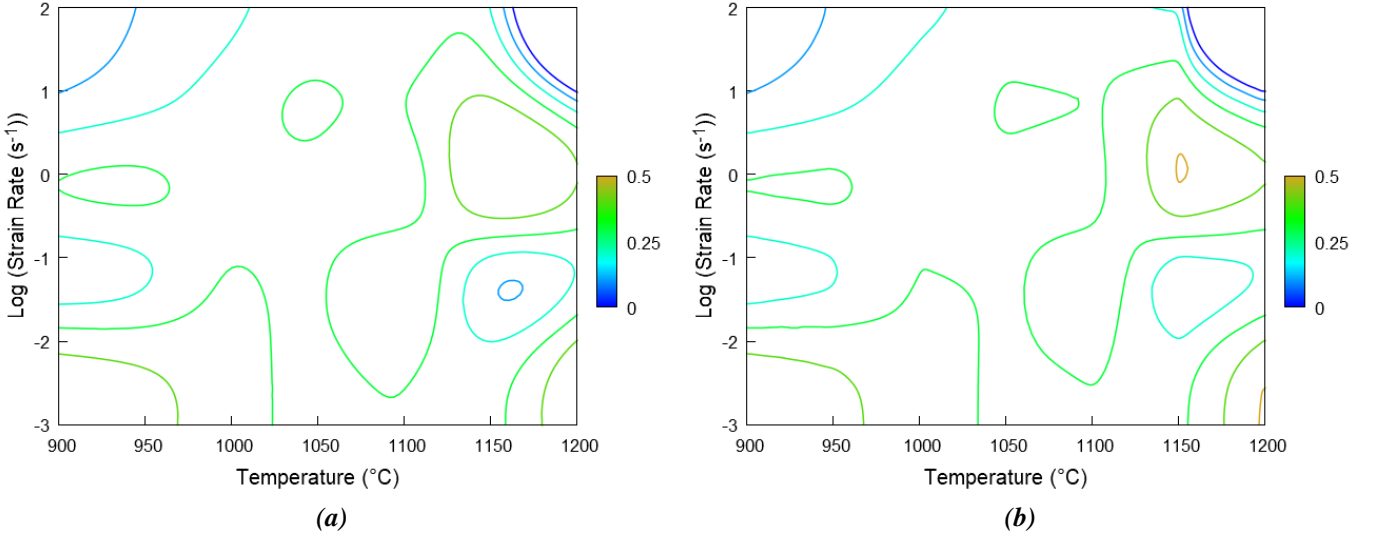


**Figure 1:** Power dissipation maps obtained for superalloy IN718 from measured flow stress at a fixed strain of 0.5.<sup>[3]</sup> The JMatPro® implementation (a) agrees well with the work of Ref. 3 (b).

where  $m$  denotes the strain rate sensitivity parameter:<sup>[3]</sup>

$$m = \frac{\partial \ln \sigma}{\partial \ln \dot{\epsilon}} \quad (6)$$

The difference between conditions (4) and (5) is in the underlying form of the flow stress versus strain rate curve. The Kumar-Prasad instability criterion assumes a power law relationship,

$$\sigma \propto \dot{\epsilon}^m \quad (7)$$

while the Murty-Rao one works for arbitrary curves.<sup>[3,4]</sup> When using the Kumar-Prasad criterion to outline the regions of unstable flow, the efficiency of power dissipation is also often calculated with the above constraint (Eq. 7).<sup>[1,4]</sup> In the JMatPro® implementation, however, the more general equation (3) is always used to determine the power dissipation map. This follows closely the work of Murty et al.<sup>[3]</sup> and calculated results from the same data agree well with those of Ref. 3, as illustrated in Fig. 1 for the nickel-iron-based superalloy IN718 (Ni-0.5Al-19Cr-18.5Fe-3Mo-5.1Nb-0.2Si-0.9Ti-0.04C wt%).

For most alloys at typical processing conditions used in hot working, the Kumar-Prasad and Murty-Rao criteria lead to similar predictions. This is exemplified in Fig. 2, which shows a comparison of the processing maps obtained considering both criteria for general steel 3310 (Fe-1.52Cr-0.45Mn-0.03Mo-3.33Ni-0.18Si-0.11C-0.03P-0.04S wt%). The JMatPro® flow stress module was used to calculate the required data to build these processing maps (typical stress-strain curves are also shown in Fig. 2).

Alternative criteria may be developed on the basis of Lyapunov's stability theory, with Lyapunov functions built from quantities introduced in the dynamic materials model. This approach leads to the Gegel and Alexander-Malas criteria,<sup>[3,4]</sup> respectively given by

$$\xi_G = \begin{cases} m < 0 \\ -\frac{\partial \eta}{\partial \ln \dot{\epsilon}} < 0 \\ s - 1 < 0 \\ -\frac{\partial s}{\partial \ln \dot{\epsilon}} < 0 \end{cases} \quad (8)$$

and

$$\xi_{A-M} = \begin{cases} m < 0 \\ -\frac{\partial m}{\partial \ln \dot{\epsilon}} < 0 \\ s - 1 < 0 \\ -\frac{\partial s}{\partial \ln \dot{\epsilon}} < 0 \end{cases} \quad (9)$$

where  $s$  is the temperature sensitivity of flow stress,<sup>[3]</sup> defined as

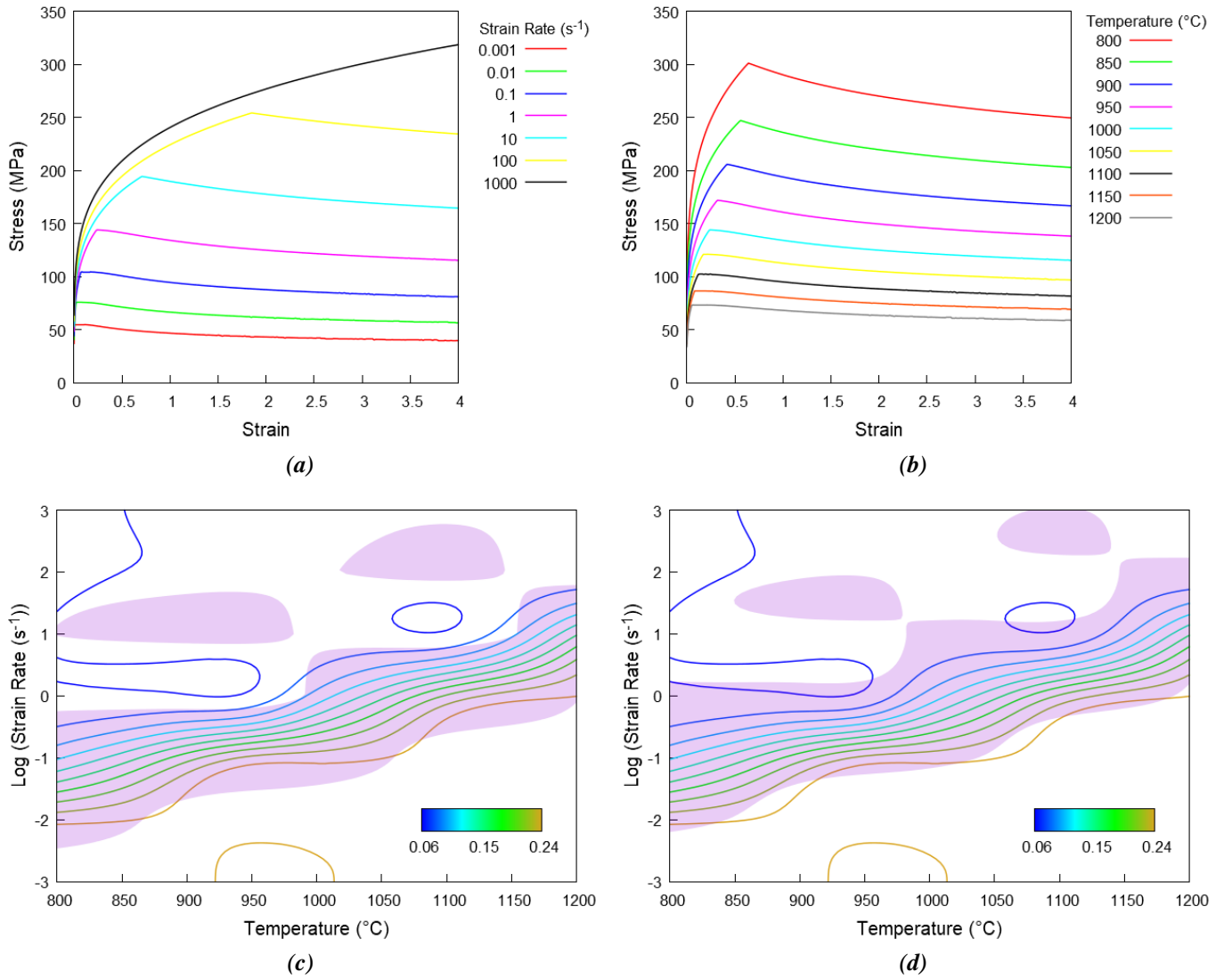


**Figure 2:** The top panels show flow stress curves calculated for general steel 3310 at a fixed temperature of 1000 °C (a) and a fixed strain rate of 1 s<sup>-1</sup> (b). The bottom panels show processing maps derived from such data at a fixed strain of 0.1. The coloured lines are isoefficiency contours, while the shaded areas are regions of unstable flow predicted using the Kumar-Prasad (c) and Murty-Rao (d) instability criteria.

$$S = \frac{1}{T} \frac{\partial \ln \sigma}{\partial (1/T)} \quad (10)$$

The only difference between criteria sets (8) and (9) is in the second condition, with  $\eta$  in the Gegel version replaced by  $m$  in the Alexander-Malas case. Again, for processing parameter ranges typical of hot working, the regions of unstable flow predicted by the Gegel and Alexander-Malas criteria sets are very similar, as illustrated in Fig. 3 for general steel 3310.

The JMatPro® module that deals with the calculation of processing maps allows the user to select one of the instability criteria discussed here, but further possibilities exist.<sup>[3]</sup> It is important to stress that none of the existing criteria is generally applicable to every material type and, in some cases, they can lead to contradictory predictions, as can be seen by comparing the processing maps of Figs. 2 and 3. The contradictory nature of various calculations has been reported previously in the literature<sup>[4]</sup> and care needs to be taken when choosing which criterion to use.

## Summary

Modelling of processing maps is a subject that has drawn some controversy. There are doubts about both the rigorousness of the analytical approach and the correctness of the predicted results.<sup>[5,6]</sup> The situation is not helped by the fact that different instability criteria may give rather different instability regions when

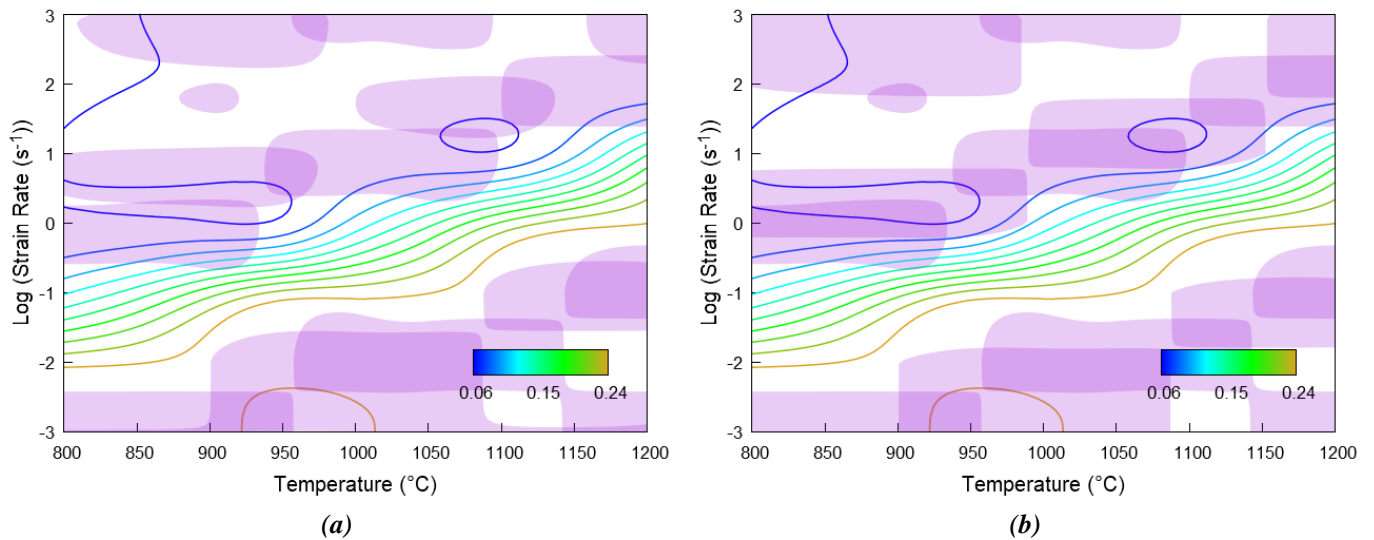


**Figure 3:** Processing maps obtained for general steel 3310 from calculated flow stress at a fixed strain of 0.1. The coloured lines are isoefficiency contours, while the shaded areas are regions of unstable flow predicted using the Gegel (a) and Alexander-Malas (b) instability criteria.

calculated from the same set of flow stress curves.<sup>[4]</sup> Therefore, the selection of which instability criterion is used and the interpretation of flow instability from the subsequently calculated processing map need to be approached with caution. Nonetheless, processing maps appear to be seen as useful tools and are quite widely used and applied to various types of alloys, e.g., steels,<sup>[7]</sup> titanium,<sup>[8]</sup> aluminium,<sup>[9]</sup> and magnesium alloys.<sup>[10]</sup> As such we have included the capability to calculate them in JMatPro®.

## References

1. Y. V. R. K. Prasad, K. P. Rao, and S. Sasidhara (editors), *Hot Working Guide: A Compendium of Processing Maps*, ASM International: Ohio (2015)
2. V. V. Kutumbarao and T. Rajagopalachary, "Recent developments in modeling the hot working behavior of metallic materials", *Bulletin of Materials Science* **19**, 677 (1996)
3. S. V. S. N. Murty, B. N. Rao, and B. P. Kashyap, "Instability criteria for hot deformation of materials", *International Materials Reviews* **45**, 15 (2000)
4. X. Wang, Z. Liu, and H. Luo, "Hot deformation characterization of ultrahigh strength stainless steel through processing maps generated using different instability criteria", *Materials Characterization* **131**, 480 (2017)
5. S. Ghosh, "Interpretation of microstructural evolution using dynamic materials modeling", *Metallurgical and Materials Transactions A* **31**, 2973 (2000)
6. S. Ghosh, "Interpretation of flow instability using dynamic material modeling", *Metallurgical and Materials Transactions A* **33**, 1569 (2002)
7. S. Venugopal, S. L. Mannan, and Y. V. R. K. Prasad, "Processing map for hot working of stainless steel type AISI 316L", *Materials Science and Technology* **9**, 899 (1993)
8. X. Ma, W. Zeng, K. Wang, Y. Lai, and Y. Zhou, "The investigation on the unstable flow behavior of Ti17 alloy in  $\alpha+\beta$  phase field using processing map", *Materials Science and Engineering A* **550**, 131 (2012)
9. H. E. Hu, X. Y. Wang, and L. Deng, "Comparative study of hot-processing maps for 6061 aluminium alloy constructed from power constitutive equation and hyperbolic sine constitutive equation", *Materials Science and Technology* **30**, 1321 (2014)
10. S. Anbuselvan and S. Ramanathan, "Hot deformation and processing maps of extruded ZE41A magnesium alloy", *Materials and Design* **31**, 2319 (2010)